Available online at www.sciencedirect.com
SCIENCE DIRECT®
Journal of Nuclear Materials 334 (2004) 180–188
journal of nuclear materials
www.elsevier.com/locate/jnucmat

Influence of dynamic strain aging on the dislocation structure developed in Zircaloy-4 during low-cycle fatigue

I. Alvarez-Armas *, S. Hereñú

Instituto de Física Rosario, CONICET, Universidad Nacional de Rosario, Bv. 27 de Febrero 210 bis, 2000 Rosario, Argentina

Received 14 November 2003; accepted 2 June 2004

Abstract

Low-cycle fatigue tests between 573 and 873 K were carried out with a total strain range of 1% in order to study the cyclic behaviour and dislocation structure developed in Zircaloy-4. According to them, three ranges of temperature have been distinguished: low, intermediate and high. The intermediate one is characterized by the activation of a dynamic strain aging process which is manifested mechanically by an incremental rate of cyclic hardening and microstructurally by a pronounced increase in the dislocation density. In order to analyse the dislocation dynamics on the evolution of the microstructure, interrupted tests have been performed. These results have been used to propose a model of dislocation glide and accumulation for a hexagonal metal.

1. Introduction

An interesting point to consider, when engineering materials are subject to deformation at certain temperatures and strain rates, is the mechanical and microstructural response caused by the activation of an atomic process such as dynamic strain aging (DSA). Numerous studies concerning this subject have revealed a modification in the dislocation slip modes. Most of the papers [1–4] related to DSA during fatigue showing drastic changes in the dislocation structure evolution have been carried out in cubic materials. However, there are only few specific studies on hexagonal-close-packed (hcp) materials concerning this effect of the microstructure evolution [5]. Few years ago [6], a work appeared in the literature containing maps of different dislocation structures developed during fatigue in a wide range of temperatures and total strain. However, neither the activation of an atomic process nor the influence of the strain rate on the dislocation structure formation was considered.

As it is well known, in the case of both body-centred cubic and hcp metals the dislocation glide depends sensitively on temperature, strain rate, and (interstitial) impurities as well as the sense of deformation. In a previous paper [7], the effect of strain rate on the cyclic behaviour of Zircaloy-4 in the DSA region was studied but not its influence on the dislocation evolution. Therefore, the aim of this work is to evaluate the influence of the temperature and strain rate on the dislocation structure evolution of an hcp material which presents anomalous cyclic behaviour as well as to establish whether there is a drastic change in the dislocation structure during DSA. Moreover, a possible dislocation mechanism for the formation of the dislocation structure is proposed when two primary slip systems are activated in a hexagonal metal.

* Corresponding author. Tel.: +54 341 485 3200; fax: +54 341 482 1772.
E-mail address: alvarez@ifir.edu.ar (I. Alvarez-Armas).

0022-3115/$ - see front matter © 2004 Elsevier B.V. All rights reserved.
doi:10.1016/j.jnucmat.2004.07.002

2. Experimental procedure

Shallow hour-glass shaped specimens were machined from Zircaloy-4 bars, prepared in accordance with ASTM B550 Grade 704. The chemical composition of the alloy in weight percent is: Sn: 1.37; Fe: 0.14; Cr: 0.10; C: 0.01; O: 0.14; N: 0.004; H: 20 ppm; Zr: balance. In general, the texture of extruded zirconium bars is such that the prismatic direction extends close to or along the rod axis and the basal direction nearly perpendicular to this axis. Thus, the initial grain orientation most probably found is in the $\langle 11\bar{2}0\rangle$ and $\langle \bar{1}100\rangle$-directions, parallel to the loading axis.

Total strain-controlled cyclic tests in the temperature range 573–873 K were carried out using a fully reversed triangular wave on a Type 1362 Instron machine. The total strain range used was $\Delta\varepsilon_t = 1\%$ and the strain rates $\dot{\varepsilon} = 2 \times 10^{-3}$ and 2×10^{-4} s^{-1}. In addition to this series, a dynamic test controlling the plastic strain range was performed with $\dot{\varepsilon} = 2 \times 10^{-3}$ s^{-1} from room temperature to 793 K. The plastic strain range was $\Delta\varepsilon_p = 0.57\%$ which corresponds nearly to the range attained during the standard tests. The test was stopped for each change of temperature after periods of 50 cycles.

In order to correlate the mechanical behaviour with the dislocation structure of fatigued specimens, interrupted tests have been performed at a certain number of cycles. The details of these tests will be specified along the section 'Results'. Thin foils have been prepared from discs mainly cut perpendicular to the tensile axis of the specimen. However, in the case of interrupted tests performed at 713 K, the microstructure has also been observed from discs cut parallel to the tensile axis taking advantage of the texture exhibited by this material. The discs were electropolished at a temperature of 253 K in a solution of 10% perchloric acid, 35% *n*-butanol and 55% methanol and observed in a Philips EM 300 transmission electron microscope operating at 100 kV.

3. Results

3.1. Mechanical behaviour

The cyclic response of Zircaloy-4 between 573 and 873 K is represented in Fig. 1. The cyclic behaviour at 573 K shows a rapid initial hardening followed by a smooth decrease of the peak tensile stress followed by a long saturation stage which lasts until rupture.

In the intermediate range of temperatures from 673 to 758 K, a completely different cyclic response of the material at the present mechanical conditions can be observed. Armas et al. [8] have reported this behaviour and attributed it to DSA manifestations. The three stages in which each curve has been divided in this temperature range are: a transitional cyclic hardening stage with a high but decreasing hardening rate; a principal hardening stage with a noticeable linear dependence of the peak tensile stress with the number of cycles, and a third stage with a decreasing rate of hardening where the peak stress attains a maximum and then falls drastically until failure. In fact, the linear hardening stage attains the minimum and the maximum values of the cyclic hardening rate at 623 and 773 K, respectively (for clarity reasons the curves corresponding to these temperatures have not been included in Fig. 1). Between 743 and 773 K, the third stage is characterized by the formation of a kind of plateau where the peak tensile stress remains almost constant.

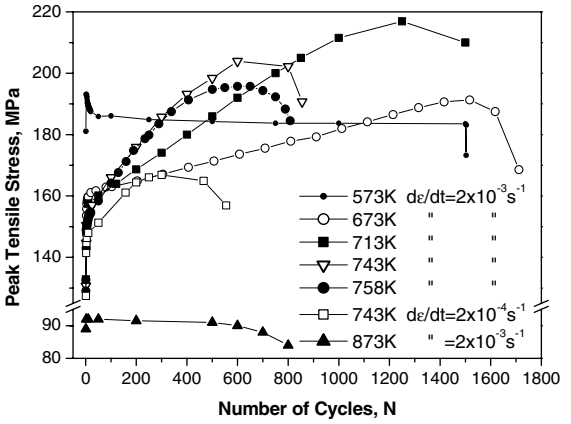

Fig. 1. Cyclic response of Zircaloy-4 for a total strain range of $\Delta\varepsilon_t = 1\%$ between 573 and 873 K.

Finally, at 873 K, the peak tensile stress remains constant after the first cycle nearly up to rupture. The level of stress lies approximately 50% lower in comparison with the level of stress reached by the curves in the intermediate range of temperatures.

Fig. 2 shows the effect of temperature on the peak tensile stress at certain numbers of cycles. This set of curves has been represented by the cyclic data of Fig. 1 as well as additional data at other temperatures such as 623, 773, 793 and 823 K. The curve corresponding to cycle 1 represents the temperature dependence of this flow stress. This curve shows, between 673 and 743 K, one of the typical aspects of static strain aging in tensile tests, i.e. an independence of the flow stress with temperature. Besides, after few cycles, this effect appears more pronounced and starts at a lower temperature (623 K). It is interesting to note for the following analysis the high values of peak tensile stress that occurs above 50 cycles around 743 K (the maximum is at 500 cycles).

Finally, in order to evaluate the atomic process activated in this material at intermediate temperatures, two additional tasks have been performed. Firstly, a plastic strain-controlled fatigue test has been carried out at

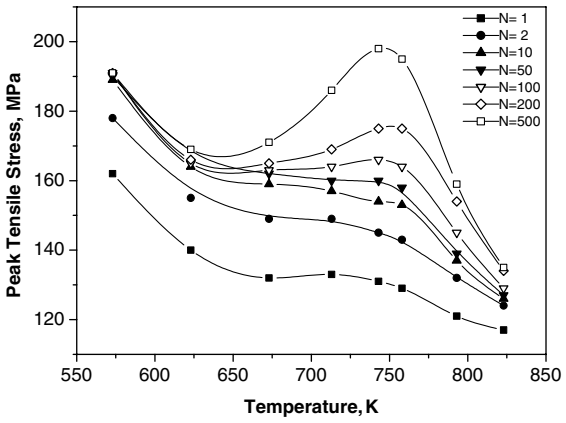

Fig. 2. Behaviour of the peak tensile stress vs. temperature for a certain number of cycles.

the fixed plastic strain range of 0.57% which was interrupted and cycled at different temperatures. Fig. 3 shows the decrease in the temperature dependence of the peak tensile stress. This curve is characterized by a pronounced plateau between 623 and 743 K where the flow stress behaves independent of the temperature. Besides, in a smaller band of temperatures between 673 and 743 K, serrations have been observed during fatigue in the stress–strain loops. It is interesting to note that 573 K appears as the threshold temperature for the activation of the dynamic strain aging. Secondly, a detailed analysis of the flow stress components as originally suggested by Cottrell [9] and employed by Kuhlmann-Wilsdorf and Laird [10] and Hanfield and Dickson [11] was used to explain the cyclic behaviour. Upon this method, the flow stress obtained from the hysteresis loops is the result of two kinds of resistance to plastic deformation: the friction σ_f and the back stress σ_b. The former corresponds to the resistance that dislocations have to overcome to keep moving, while the back stress is associated with a 'hard' dislocation structure that cannot be overcome with the assistance of temperature. Fig. 4 shows the behaviour of these components at 758 K and $\dot{\varepsilon} = 2 \times 10^{-3}$ s^{-1}. It is interesting to observe that the flow stress follows the behaviour of the back stress all the time, while the friction stress remains almost constant from the beginning.

3.2. Microstructural behaviour

In order to avoid a huge extension of the paper, only those micrographs with relevant importance to follow the analysis during the discussion will be exhibited here. The micrographs which have been already published anytime will be quoted and simple structures will be just described.

Fig. 5 shows a square-shaped cell structure developed at rupture at 573 K which consists of two sets of walls, one perpendicular and the other parallel to a primary slip direction $\langle 11\bar{2}0 \rangle$-type. The former arrangement is composed of bundles of edge dipoles and the latter one of entanglement of jogged screw components and many elongated loops with their longest axis perpendicular to a primary slip system. Additionally, other grains in the same specimen have shown a higher degree in the development of this cell structure containing refined walls with a relatively low density of dislocations.

Within the intermediate temperatures, those which exhibit a relatively longer principal stage such as 673 and 713 K, the dislocation arrangement is associated

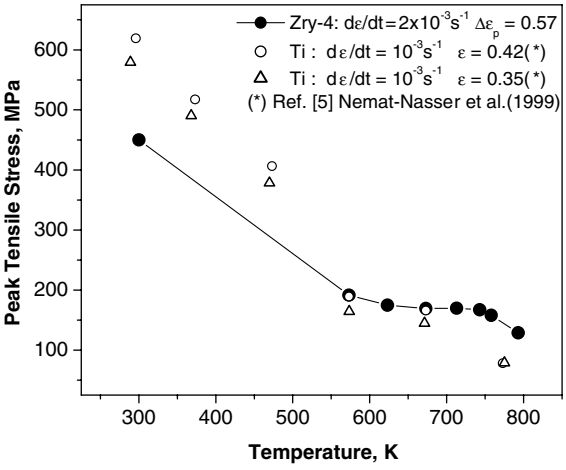

Fig. 3. Behaviour of the peak tensile stress vs. temperature for a plastic strain range of $\Delta\varepsilon_p = 0.57\%$. It shows a plateau where DSA is activated.

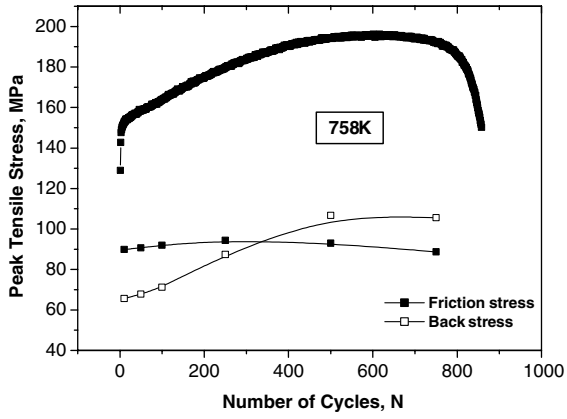

Fig. 4. Friction and back stresses at 758 K for a strain rate of $\dot{\varepsilon} \times 10^{-3}$ s^{-1}.

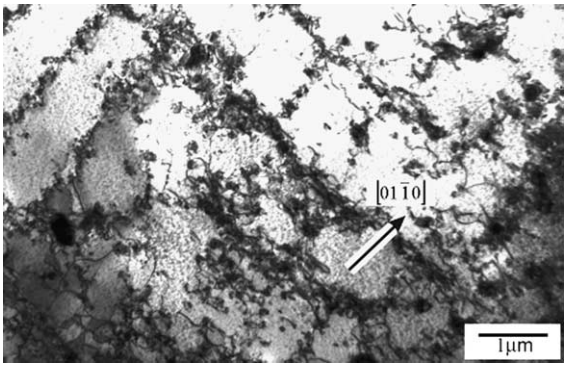

Fig. 5. Dislocation structure observed at 573 K at rupture, $\mathbf{B} \approx [01\bar{1}0]$.

with a three-dimensional structure which appears as the most compact and densest structure from all that were observed in other temperatures as was previously reported [12]. Depending on the crystallographic orientation, the structure shows either dipolar bundles oriented perpendicular to the primary slip direction separated by very narrow channels or the entire structure that consists of square-shaped cells aligned along a primary slip direction. On the other hand, above 758 K, where the cyclic curve presents a more extended third stage, the dislocation structure has the same aspect as that just described but the dislocation density is substantially lower [8]. From here on, the structure associated with the principal or linear stage will be referred as 'hard structure' while that one developed during the extended third stage will be referred as 'recovered structure'.

In order to analyse the evolution of the dislocation structure with the number of cycles, interrupted tests have been carried out for a representative number of cycles. For this purpose, two temperatures have been chosen, 713 and 758 K. Whereas the former temperature exhibits a cyclic curve with a longer linear hardening stage in relation to its third stage, at the other temperature on the contrary, the third stage is longer than the linear one (Fig. 1). At 713 K, the number of selected cycles was: 1, 10, 50 and 500. The first cycle ($N = 1$) gives information about the first mechanism activated after the process of tension and compression (stopped at $\sigma = 0$) in the present thermomechanical conditions. The cycle number 10 ($N = 10$) is representative of the microstructure formed during the transitional cyclic hardening stage, while the cycle number 50 is representative of the evolution that has to undergo the initial dislocation structure to attain the second or principal hardening stage. Finally, the dislocation structure developed at 500 cycles represents the microstructure of the principal hardening stage by which the material reaches high values of peak tensile stress and, according to Fig. 2, the maximum effect of the DSA. At 758 K, the test has been only interrupted at 400 cycles since it represents the onset of the extended third stage where a recovery process will occur.

After the first cycle, at 713 K, many edge dipoles can be observed in the matrix gathering together in incipient dipolar walls (see Fig. 6(a)). At 10 cycles (Fig. 6(b)), the microstructure reveals a more complicated process. Indeed, the first dipolar walls coarsen accumulating more and more dipoles, while an increasing number of screw components and a great deal of small and elongated loops oriented perpendicular to the slip direction form part of the microstructure. A detailed analysis of the microstructure has shown the presence of numerous screw components containing trails of two edge dislocations, i.e. dislocation dipoles, as well as the pinching-off of the dipole-trails forming loops. Besides, jogged screw dislocations could be detected through the bowed out of the dislocation in one point.

For the next number of cycles, namely 50 and 500 cycles, the dislocation structure has been analysed from two perpendicular directions, one parallel and the other perpendicular to the tensile axis of the specimen.

As it was already mentioned, after approximately 50 cycles the material suffers a decrease in the cyclic hardening rate followed then by a linear dependence of

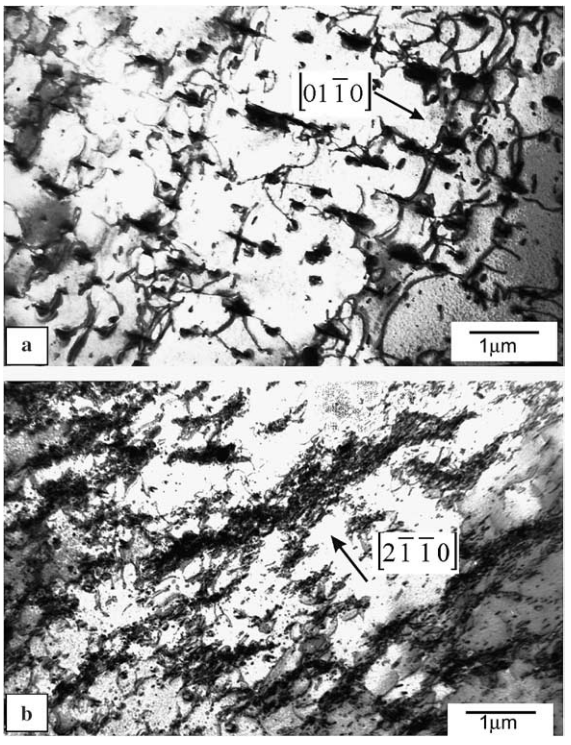

Fig. 6. Dislocation structure at 713 K: (a) $N = 1$ cycle incipient dipolar walls, $\mathbf{B} = [2\bar{1}\bar{1}0]$, (b) $N = 10$ cycles bundles of edge dipoles and tiny loops, $\mathbf{B} = [01\bar{1}1]$.

the peak tensile stress with the number of cycles. This change in the cyclic behaviour is associated with the activation of a second slip system. Fig. 7(a) and (b) show two different dislocation structures developed until this point in two well apart crystallographic orientations, from $\mathbf{B} = [\bar{1}2\bar{1}6]$ (30° from the basal direction, Fig. 7(a)), and from $\mathbf{B} = [0\bar{1}10]$ (prismatic-direction, Fig. 7(b). The former one corresponds to bundles of edge dipoles and loops as well as long straight screw dislocations linking bundles. They frequently present nodes with the formation of quadrupoles as a result of the intersection of screw dislocations in different slip systems. The latter one shows a square-shaped cell arrangement of dislocations composed of bundles of edge dipoles organised perpendicular to the $[2\bar{1}\bar{1}0]$-axis and strings of small elongated loops lined up along this direction (incipient second set of walls). The distance between this second set of walls is about 1000 nm. Then, the structure formed at this stage of the fatigue life can be considered as the formation of the square-shaped cell structure. Fig. 8 shows the dislocation structure developed at 500 cycles where the final square-shaped cell structure is formed. The morphology of the dislocation structure does not change in comparison with that of 50 cycles but the dislocation density is much more pronounced and heterogeneously distributed. At this number of cycles, the average distance between walls of the second set is reduced as a consequence of the increase in the dislocation density, and reaches an average value of about 600 nm. It is important to remark that this value has been calculated after measuring over 20 micrographs. Besides, a statistical estimation of the separation between trails of the two edge dislocations which form the dipole in a jogged screw dislocation has thrown a value of 30 nm.

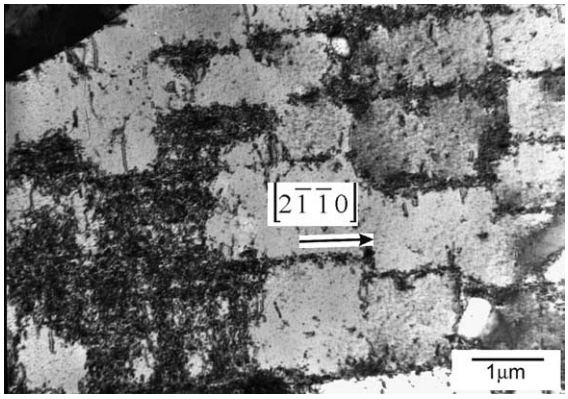

Fig. 8. Square-shaped cell structure developed at 713 K and 500 cycles observed from $\mathbf{B} = [01\bar{1}0]$.

The next step in this analysis is to consider what happens with the hard dislocation structure formed during the linear stage when an extended third stage takes place. Fig. 9 shows the dislocation structure observed at 758 K when the linear stage comes to the end and starts the plateau (at 400 cycles). This structure is characterized by the combination of two ones: the right part

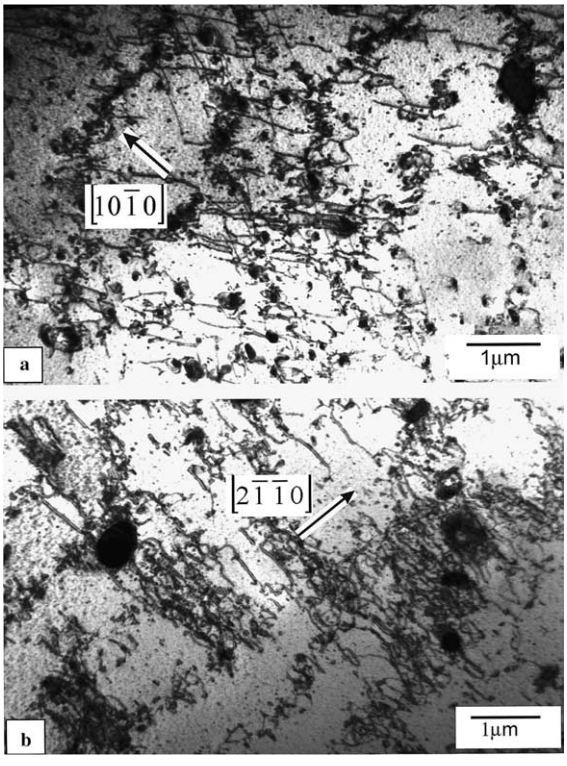

Fig. 7. The observed dislocation structure at 713 K and 50 cycles: (a) **B** close to $[\bar{1}2\bar{1}6]$ reveals a structure of bundles of edge dipoles and some quadrupoles, (b) $\mathbf{B} = [01\bar{1}0]$ shows the formation incipient square-shaped cell structure.

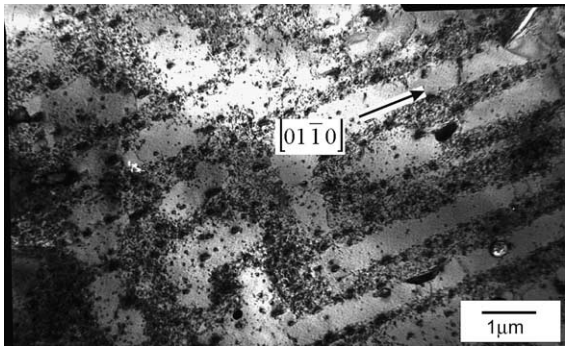

Fig. 9. A mixed dislocation structure is observed at the end of the linear stage at 758 K, $N = 400$ cycles. It is composed of both the square-shaped cell structure typical of that stage and the band structure typical of the high temperature regime, $\mathbf{B} = [2\bar{1}\bar{1}0]$.

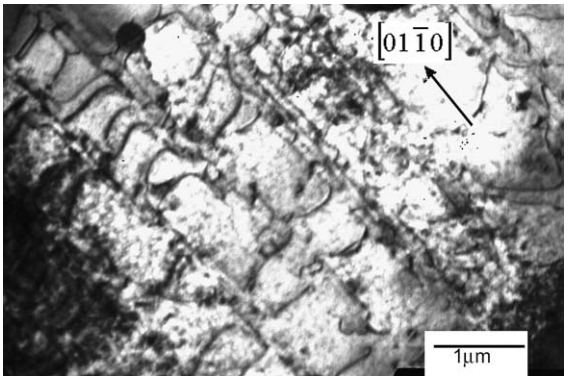

Fig. 10. Band dislocation structure developed at 743 K with a strain rate of $\dot{\varepsilon} \times 10^{-4}$ s^{-1}.

composes of a dislocation arrangement parallel to a slip direction, while the left part contains the square-shaped dislocation structure considered above.

Finally, Fig. 10 shows an example of the final dislocation arrangement developed in the intermediate range of temperature with the slowest strain rate – that is $\dot{\varepsilon} = 2 \times 10^{-4}$ s^{-1}. In particular at 743 K, the cyclic curve presents an extended third stage after a short linear stage. The dislocation arrangement observed at this level corresponds to a well formed dislocation band structure parallel to the primary slip direction. The striking feature in this dislocation structure is the absence of the edge dislocation arrangement.

4. Discussion

4.1. Evolution of the dislocation structure with temperature

The result of the microstructural observations performed in all the temperature range has shown that the material develops basically a square-shaped cell structure between 573 and 773 K. Nevertheless, the most important difference of this structure at different temperatures lies in the dislocation density. At intermediate temperatures where DSA occurs, the dislocations appear not to be able to leave the glide plane and progressively accumulate in the structure. Thus, a planar mode characterizes the dislocation glide in this region of temperatures. Above and below this range, a recovery process takes place and modifies the level of stresses imposed to the material.

The cyclic behaviour at 573 K shows high values of the peak tensile stress during the first cycles and then decreases until the saturation occurs. This stage of stabilization in almost all the fatigue life suggests a balance in the production and annihilation of dislocations during cycling. In fact, many grains have shown a recovered state of dislocation cells at the end of the fatigue life. On the other hand, the results of Fig. 3 clearly show that already the temperature of 573 K appears as the threshold where DSA is activated. In fact, this is a more precise method to determine the beginning of the phenomenon. Armas et al. [13] have shown in a previous paper through static heat treatment in Zircaloy-4 that this temperature promotes the diffusion of oxygen atoms to dislocations. Therefore, according to our microstructural results the mobility of this kind of atoms is insufficient to reach the dislocation to produce a dragging force on them.

The process of DSA is activated during deformation between 623 and 773 K, as the result of Figs. 2 and 3 suggests. The same result has been observed by Nemat-Nasser et al. [5] in Ti. For comparison reasons some data of that paper obtained under similar mechanical conditions were included in Fig. 3. The similarity of the flow stress values of both materials in the DSA region is remarkable. According to the experimental results published by many authors [13–16], the atom in question is oxygen which can move to dislocations at appropriate temperature and strain rate producing the subsequent drag force on dislocation movement. Taking this into account, the dislocation density increases during cycling raising the peak tensile stress of the material (see Fig. 2).

Within the same range of temperatures, 758 K appears as the upper limit which defines the end of the DSA process. Comparing the cyclic curves at 758 and 743 K, it is interesting to note that the relative duration of the linear stage at 758 K is shorter even though both curves have identical rates of cyclic hardening during the linear stage (Fig. 1). Thus, the combination of the higher temperature with high stresses inhibits the effect of DSA releasing dislocations from the atoms and allowing them to cross to another plane. The result of Fig. 4 shows that the linear stage is associated with an incremental rate in the back stress that can be explained by the subsequent accumulation of dislocations at the structure, Fig. 8, while the third stage is connected with a balance in the creation and annihilation of dislocations, Fig. 9. This fact is represented by the dislocation structure during the transition from the second to the third cyclic stage ($N = 400$ c). It exhibits a softer dislocation structure where the dislocation density has been diminished due to the activation of the cross-slip process as it was analysed previously. It is interesting to note that the structure on the right of the micrograph is similar to that reported in a previous paper [17] cycled under the same mechanical conditions, but at 873 K. This structure was described as a band structure homogeneously distributed which runs from border to border of a grain without interruption and separated by channels with a considerable low density of edge dislocations. The cyclic

curve associated with this structure can be observed in Fig. 1 and is characterized by an extended saturation stage after few initial cycles to attain the regime. The main crystallographic feature of this structure was the activation of the cross-slip process to pyramidal planes of the type $\{1\bar{1}01\}$ and the annihilation of edge dislocations by climb. Similar analysis carried out on the present structure and observed on the right side of Fig. 9 has shown the process of cross-slip on the same type of planes.

4.2. Model of dislocation glide and accumulation

The analysis of the microstructure at intermediate temperatures shows that the dislocation distribution during the first cycles follows the ordinary process proposed in the literature [18] which is characterized by the entanglement of primary edge dipoles in bundles. However, the onset of the principal cyclic stage is associated with the activation of a second prismatic slip system being now relevant to the contribution of the screw dislocations in the microstructure. Indeed, the main contribution of these components in the present material is the formation of loops as was observed in Fig. 7(b).

Hereafter, a model of dislocation glide and accumulation that results in the formation of a square-shaped cell structure in an hcp metal is proposed. It takes into account the formation of a second set of walls composed principally of elongated loops of mixed character align along a $[11\bar{2}0]$-direction as well as the presence of straight long screw dislocations linking bundles. This model is in accordance with the two different views of the three-dimensional structure for the two well apart crystallographic directions, Fig. 7. Lastly, the stress generated within a cell of this structure formed at 713 K and after 500 cycles will be calculated, where the DSA exerts a strong influence, in order to evaluate the possibility of loop formation after this model.

The mechanism of the dislocation dynamics at the beginning of the linear hardening ($N \approx 50$ c) involves the activation of two primary slip systems of the type $\{1\bar{1}00\}$ $[11\bar{2}0]$ with different Burgers vectors $\boldsymbol{b_1}$ and $\boldsymbol{b_2}$. Since these vectors are not orthogonal the dislocation lines will exert long range elastic interactions each other [19]. When two screw dislocations on different slip planes meet at a point their intersection can result in the formation of a quadruple point. On the other hand, the intersection of a screw dislocation (segments ABCD) with an edge dislocation (segments WXYZ) on different prismatic planes, $(10\bar{1}0)$ and $(01\bar{1}0)$, respectively, produces an elementary jog (BC and XY, respectively) in each dislocation of length or 'height' equal to the Burgers vector of the intersecting dislocation as it is shown in Fig. 11. As a consequence of the hexagonal geometry of the crystal involved, the resultant jog on the screw dislocation (BC) does not form a right angle with the dislocation line while that acquired by the edge dislocation (XY) does. As the jog on a screw dislocation has edge character and as an edge dislocation can glide freely only in the plane containing its line and Burgers vector, the only way the jog can move by slip is along the axis of the screw dislocation. Therefore, the dislocation can

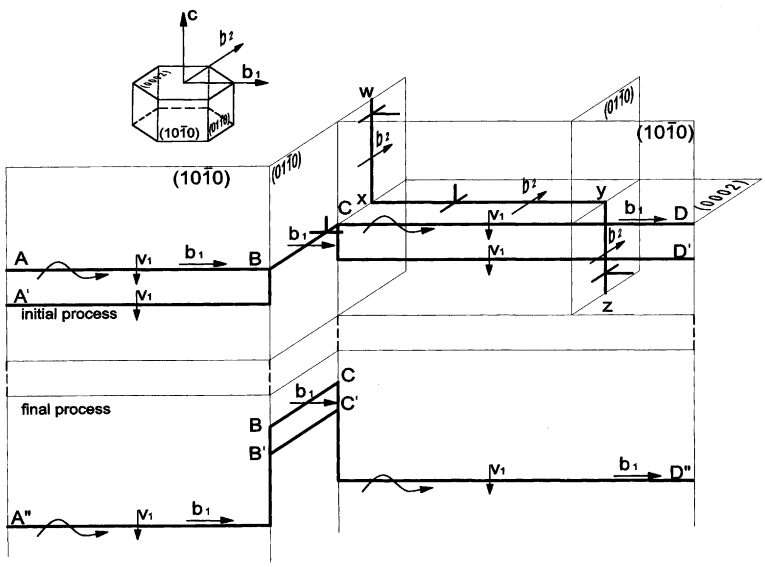

Fig. 11. Schematic illustration of the dislocation dynamics in an hcp metal when two primary slip systems are activated. The intersection of a screw with an edge dislocation produces the formation of sessile loops on the prismatic plane which are of mixed character.

move forward and take the jog with it only non-conservatively. In the case of the edge dislocation, the segment (XY) of dislocation which forms the jog lies on the basal plane being this a compact plane favourable to glide. According to this analysis, jogged screw dislocations would move, non-conservatively, either with the assistance of interstitial atoms or creating vacancies. The result of the non-conservative motion of jogged screw dislocations produces the formation of elongated loops (BCC′B′) on a prismatic plane which are not of pure edge character. This feature will be one of the key factors in the recovery process observed under different thermomechanical conditions because the screw part will be able to glide to another plane by cross-slip allowing thus the process of recovery. On the other hand, these loops may break up into smaller loops in order to reduce its energy. The movement of jogged screw dislocations leaving behind strings of sessile loops would explain the great deal of dislocation loops aligned along the $[1\,1\,\bar{2}\,0]$-direction displayed in the dislocation structure (forming the second set of walls) projected on the prismatic plane at 50 cycles.

Regarding the different views of the three-dimensional structure, let us start with the arrangement developed during the first cycle. It consists of small bundles of edge dipoles on the primary prismatic plane, whose projection presents identical characteristics either on a basal or prismatic plane. However, as cycling proceeds, a second slip system is activated with the subsequent formation of the second set of walls containing loop arrangements as well as the corresponding bundles of edge dipoles on the second set of prismatic planes. Therefore, the overall three-dimensional structure is very different in different orientations. In the prismatic section, which coincides with one slip plane, the structure exhibits two sets of walls, one parallel and the other perpendicular to a slip direction. In the basal section, the structure is associated with dense bundles of dipoles and loops aligned nearly perpendicular to a slip direction. From this orientation the loop strings which form the second set of walls remain hidden by the dipolar structure.

Finally, an estimation of the level of stress within the free areas of the dislocation structure will be performed. According to Derep et al. [20] the shear stress τ corresponding to the applied stress is obtained from the following relationship:

$$\tau = \sigma_{0.02}/M, \tag{1}$$

where $\sigma_{0.02}$ is the applied stress and M the average Taylor factor which relates the normal strain rate $\dot{\varepsilon}$ to the shear strain rate $\dot{\gamma}$ in the glide plane. Luton and Jonas [21] have assumed that M is equal to 4. Once the preliminary structure is formed (around 50 cycles), the mean free path Λ for dislocations corresponds to the distance between dislocation walls. Thus, the flow stress [22] required to bend a dislocation to a radius $1/2\Lambda$, is:

$$\tau_\Lambda \simeq G \cdot b/\Lambda, \tag{2}$$

where G is the shear modulus and b is the Burgers vector. Moreover, the interaction stress between the two parallel edge dislocations of opposite sign which are associated with a dipole formed on a screw dislocation as a result of a jog formation is given by the following expression:

$$\tau_d = \frac{0.25\ G \cdot b}{2\pi(1-\nu)y}, \tag{3}$$

where y is the height of the jog and ν is the Poisson number.

Some typical values for Zry-4 are: $G = 35$ GPa, $b = 0.332$ nm, $\nu = 0.33$. Taking values of the applied flow stress σ_a, the height of the jogs y and the distance between the cell walls Λ of the experiment carried out at 713 K for $N = 500$ cycles, $\tau = 50$ MPa, $y = 30$ nm and $\Lambda = 600$ nm. According to these values the bending stress for dislocation in the interior of a cell corresponds to $\tau_\Lambda = 20$ MPa while the interaction stress between dislocations in the dipole was estimated at $\tau_d = 23$ MPa. Therefore, after this simple calculation, it is possible to expect that only jogs with a height less or equal to 30 nm are able to form loops, but those with higher distance will form dipole trails whose dislocations will move independently.

4.3. Influence of the strain rate on the evolution of the dislocation structure

More insight into the study of the evolution of the dislocation structure in Zry-4 with temperature needs to consider the influence of the strain rate. As was aforementioned, the cyclic curves between 623 and 823 K are characterized by three hardening stages. The relative duration (in number of cycles) of these stages depends strongly on temperature and total strain rate as can be observed in Fig. 1. Therefore, fixing the value of the total strain rate at 2×10^{-3} s^{-1} and raising the temperature from 713 to 758 K, the duration of the second hardening stage decreases drastically. Similar behaviour was found fixing the temperature at 743 K and decreasing the value of the strain rate by one order of magnitude. This decrease in the strain rate produces a more extended third stage of about 25% according to Fig. 1. Consequently, the range of temperature where the maximum effects of DSA take place is shifted towards higher temperatures at the fastest strain rate [7]. This fact would explain why the dislocation structure observed in Fig. 9 ($T = 758$ K and $\dot{\varepsilon} = 2 \times 10^{-3}$ s^{-1}) is still a mixture of the hard and recovered structure and that of Fig. 10 ($T = 743$ K and $\dot{\varepsilon} = 2 \times 10^{-4}$ s^{-1}), at a lower temperature, has already completed the formation of the recovered structure exhibiting identical crystallographic features to that observed at 873 K. That structure was considered as a recovered one since no cyclic hardening

occurs at 873 K. In this context, Zircaloy-4 with a melting temperature of 2130 K behaves as if its melting temperature were the α–β transformation temperature [23]. If this were the case, 873 K represents a very high homologous temperature.

5. Conclusions

1. The dislocation structure developed during the low-cycle fatigue performed with a total strain range of 1% between 573 and 773 K corresponds to an unusual three-dimensional square-shaped cell structure which is not seen in cubic metals. The formation of such structure needs the activation of two primary slip systems of the type $(1\bar{1}00)$ $[11\bar{2}0]$.
2. At intermediate temperatures between 623 and 773 K, a DSA process takes place provoking a striking increase in the dislocation density. This increment originates a profound enlargement of the amount of dipole bundles and loop arrangements.
3. The planar character of the dislocation slip characterizes the regime of intermediate temperatures during linear hardening.
4. The recovery process is associated with the formation of a plateau as the third cyclic stage and takes place for certain combinations of temperature and strain rate. It is manifested by the process of cross-slip from prismatic to pyramidal planes of the type $\{10\bar{1}1\}$ in the second set of walls as well as by climb of edge dislocations in the dipolar bundles.

Acknowledgments

This work was supported by the Agencia Nacional para la Promoción de la Ciencia y Técnica (ANPYCT) and the Consejo de Investigaciones Científicas y Técnicas from Argentina. The authors wish to thank Professor and Doctor A.F. Armas for his interest and support in this work. They wish also to thank Lic. M.G. Moscato for the technical work at the electron microscope and C. Bustamante for the drawing material.

References

[1] K.B. Sankara Rao, M.G. Castelli, J.R. Ellis, Scr. Met. Mater. 33 (1995) 1005.
[2] M. Gerland, R. Alain, B.A. Saadi, J. Mendez, Mater. Sci. Eng. A229 (1997) 68.
[3] A.F. Armas, O.R. Bettin, I. Alvarez-Armas, G.H. Rubiolo, J. Nucl. Mater. 155–157 (1988) 646.
[4] H. Mughrabi, Z. Metallkd. 94 (2003) 5.
[5] S. Nemat-Nasser, W.G. Guo, J.Y. Cheng, Acta Mater. 47 (1999) 3705.
[6] L. Xiao, H. Gu, Metall. Mater. Trans. A 28 (1997) 1021.
[7] M.G. Moscato, M. Avalos, I. Alvarez-Armas, C. Petersen, A.F. Armas, Mater. Sci. Eng. A. 234–236 (1997) 834.
[8] A.F. Armas, I. Alvarez-Armas, G. Moscato, Scr. Met. Mater. 34 (1996) 281.
[9] A.H. Cottrell, Dislocations and Plastic Flow in Crystals, Oxford University Press, London, 1953, p. 111.
[10] D. Kuhlmann-Wilsdorf, C. Laird, Mater. Sci. Eng. 37 (1979) 111.
[11] L. Hanfield, J.I. Dickson, in: G.C. Sih, J.W. Provan (Eds.), Defects Fracture and Fatigue, Martinus Nijhiff, The Hague, 1983, p. 37.
[12] I. Alvarez-Armas, A.F. Armas, in: K.T. Rie (Ed.), Low Cycle Fatigue and Elasto-Plastic Behaviour of Materials, Elsevier Applied Science, 1987, p. 77.
[13] A. Armas, S. Hereñú, R. Bolmaro, I. Alvarez-Armas, J. Nucl. Mater. 326 (2003) 195.
[14] I.G. Ritchie, K.W. Sprungmann, J. de Physique. Coll. C5 (10) (1981) C5-427.
[15] S.I. Hong, W.S. Ryu, C.S. Rim, J. Nucl. Mater. 120 (1984) 1.
[16] Z. Trojanova, A. Dlouhy, P. Lukac, J. Mater. Sci. 30 (1995) 2930.
[17] I. Alvarez-Armas, A.F. Armas, R. Versaci, J. Mater. Sci. 25 (1990) 2454.
[18] C. Laird, Fatigue and microstructure, in: Proceedings of the 1978 ASM Materials Science Seminar, St. Lous, Missouri, ASM, 1979, p. 149.
[19] J. Friedel, Dislocations, Pergamon Press, 1964, p. 42.
[20] J.I. Derep, S. Ibrahim, R. Rouby, G. Fantozzi, Acta Met. 28 (1980) 607.
[21] M.J. Luton, J. Jonas, Can. Metall. Quart. 11 (1972) 79.
[22] E. Orowan, in: Symposium on Internal Stresses, Institute of Metals, London, 1947, p. 451.
[23] R.L. Keusseyan, C.P. Hu, C.Y. Li, J. Nucl. Mater. 80 (1979) 390.